

Trajectory Tracking Control of a Class of Underactuated Mechanical Systems with Nontriangular Normal Form Based on Block Backstepping Approach

Received: 27 August 2018 / Accepted: 13 January 2019 © Springer Nature B.V. 2019

Abstract

In this paper, the formulation of a block-backstepping control approach is presented to address the trajectory tracking problem for a general class of nonlinear n degrees of freedom (n-DOF) underactuated mechanical systems (UMSs) in nontriangular normal form. First, the Euler-Lagrange model of the general form of UMSs is transformed into block-strict feedback form. Then, control input for the n-DOF UMS will be obtainable by synthesis of the backstepping approach. Additionally, an integral action is incorporated to the proposed controller to enhance the steady state performance of the overall system and also to improve the trajectory tracking precision of the control system. Lyapunov theory is utilizable to prove the stability and convergence of the overall system. To demonstrate the effectiveness of the designed controller, the proposed control algorithm is applied through numerical simulation for the trajectory tracking of a single-link flexible-link flexible-joint manipulator (SFLFJM) as an UMS with the nontriangular normal form.

 $\textbf{Keywords} \ \ Under a ctuated \ mechanical \ system \cdot Trajectory \ tracking \cdot Block-backstepping \ control \cdot Flexible-link \ flexible-joint \ manipulator$

1 Introduction

An underactuated mechanical system (UMS) is referred to a mechanical system with n degrees of freedom (n-DOF) with configuration variables $q \in \mathbb{R}^n$ and conjugate momenta $p := \partial L/\partial \dot{q} \in \mathbb{R}^n$ (where L is Lagrangian), if the generalised forces, $\tau \in \mathbb{R}^m$, be such that m < n [1]. For the UMS, the degree of underactuation is equal to (n-m) [2]. In last decades, some researchers showed strong interests in the control aspects of UMSs because of their broad applications in robots of flexible-link, mobile

Mohammad-Reza Moghanni-Bavil-Olyaei

Ahmad Ghanbari a-ghanbari@tabrizu.ac.ir

mr-moghanni@tabrizu.ac.ir

Jafar Keighobadi keighobadi@tabrizu.ac.ir

Published online: 24 January 2019

Faculty of Mechanical Engineering, University of Tabriz, 29 Bahman, Tabriz, Iran

School of Engineering Emerging Technologies, University of Tabriz, 29 Bahman, Tabriz, Iran and walking types for example, aerospace vehicles such as helicopters, aircrafts, spacecrafts and satellites, marine vehicles, underwater vehicles, etc [3–5].

In the UMSs, the absence of actuation in some configuration variables causes a challenging topic to achieve the desired control objectives with only output information available. The underactuated configuration variables can only be driven by the coupling movement of actuated variables. Hence, their internal dynamics is very complicated and generally is not feedback linearizable. Collocated partial feedback linearization and also an additional change of coordinates have been proposed to transform the UMSs into the cascaded normal forms with a useful classification of UMSs [3]. On the other hand, based on actuation/passivation of shape variables, i.e. configuration variables that appear in the inertia matrix, UMSs have been classified into two classes [3]. The first class called Class-I has actuated shape variables and is in lower triangular normal form, i.e. strict feedback form or semi strict feedback form, and the second class called Class-II has unactuated shape variables and is in nontriangular normal form. A restriction of Class-II UMSs is that they have equal number of external and shape variables. This is in fact not necessary, if a collocated partially linearizing



feedback is used which linearizes the dynamics of external variables, or a non-collocated nonlinear combination of external and shape variables. In order to extend the application of Class-II systems to systems with non-equal number of external and shape variables, a global normal form for a class of UMSs with unactuated shape variables has been presented in [3]. This so-called Class-IIb of UMSs is important particularly due to its application in tracking control of flexible-link manipulators [6]. Therefore, in this classification, flexible-link manipulators are UMSs with unactuated shape variables that are classified in Class-IIb and also have nontriangular normal form [3].

On the other hand, the design of controller for UMSs is more complicated than that of a fully-actuated mechanical systems. Many of well-known control methods and also nonlinear control methods proposed for fully-actuated mechanical systems cannot be directly applied for the UMSs. Therefore, the control issue of UMSs is a challenging task and open problem to be solved and has attracted a lot of interest over the past decades [4]. Various control techniques have been developed to stabilize and design of controllers for UMSs in order to tackle with their difficulties and to control them more effectively. Most of these techniques are based on nonlinear control methods due to the lack of control input to the unactuated configuration variables [5, 7].

In last few decades, many researches have been carried out to enrich the findings in nonlinear control, and backstepping method has emerged as one of the most efficient feedback control methods for nonlinear systems [8]. Backstepping is a Lyapunov-based control design approach for nonlinear systems that guarantees the convergence of the tracking error variables to zero [9, 10]. To apply the ordinary integrator backstepping technique for a system, it is essential that the system be in the strict feedback form [11]. In general, Class-I UMSs are in lower triangular normal form i.e. strict feedback form or semi-strict feedback form and thereby, the integrator backstepping can easily be applied. However, owing to the nontriangular normal structure of Class-II UMSs, the ordinary integrator backstepping is not directly applicable in design of control system for the Class-II UMSs.

Recently, several modified backstepping algorithms have been proposed to extend the advantageous features of backstepping technique that can effectively address the control problems of more generalized class of nonlinear systems [12, 13]. Block backstepping-based algorithm as an effective backstepping technique has addressed the stabilization problem of nonlinear systems [12, 14]; however, the trajectory tracking problem of the Class-II UMSs is still an open research problem. Chang proposed a block backstepping control for a class of multi-input multi-output (MIMO) systems to solve the tracking problem [15].

Rudra et al have developed a block-backstepping based tracking control for nonholonomic wheeled mobile robot [16]. A modified block backstepping approach for trajectory tracking control of underactuated unmanned surface vessel is also applicable [17]. However, the studied methods are not directly applicable for tracking control problem of more generalized nonlinear systems.

The tracking control problem of robotic manipulators considering both the link flexibility and joint flexibility concurrently, i.e. flexible-link flexible-joint manipulators (FLFJMs), have not been investigated yet to the best of our knowledge. Hence, the control system of FLFJM, as an example of Class-IIb UMSs, is still an open problem is investigated in this research work.

Motivated by the above discussed subjects, in this paper, we introduce a novel block-backstepping method to address the trajectory tracking control of a class of *n*-DOF UMSs with nontriangular normal form. The main contributions of this paper are summarized as follows: (i) The class of UMSs with nontriangular normal form is distinguished which is called Class-II UMSs, (ii) Based on the constructed formulation for the UMSs, a block backstepping control algorithm is proposed for trajectory tracking problem and its stability is proved by means of Lyapunov theory, (iii) Eventually, the proposed control algorithm is successfully applied for the end-point tracking of the SFLFJM as an UMS of Class-IIb with 4 degrees of freedom and 3 underactuation degrees. The simulation results verify the performance of the proposed control scheme.

The remainder sections of this paper are organized as follows. Section 2 describes the problem formulation and dynamics of the UMSs with nontriangular normal form in detail. Section 3 presents the trajectory tracking control design for the class of *n*-DOF UMSs. In this Section, first, the procedure of the control law design for the UMSs is described. Next, the proof of stability for the proposed control scheme is given. In Section 4, the dynamics of a SFLFJM as a case study for the UMSs of Class-IIb is described. Section 5 presents the software simulation results of the proposed control algorithm on the SFLFJM. Finally, the concluding remarks are released in Section 6.

2 Problem Formulation

In this section, we first describe the dynamics of the n-DOF UMSs and then the transformation of its Lagrangian form to a cascade suitable form for the control system design.

We consider the general form of *n*-DOF UMSs whose dynamics can be formulated as

$$m_{xx}(q_s)\ddot{q}_x + m_{xs}(q_s)\ddot{q}_s + h_x(q,\dot{q}) = B(q)\tau$$

$$m_{sx}(q_s)\ddot{q}_x + m_{ss}(q_s)\ddot{q}_s + h_s(q,\dot{q}) = 0$$
(1)



where $q_x \in \mathbb{R}^m$ and $q_s \in \mathbb{R}^{n-m}$ show external variable and shape variable vectors, respectively. $q = [q_x \ q_s]^T \in$ \mathbb{R}^n is the configuration vector of *n*-DOF UMS. The time derivative of the configuration vector q is expressed as, $p = [p_x \ p_s]^T \in \mathbb{R}^n$. $\tau \in \mathbb{R}^m$ stands for the control input (m < n) of applicable torques or forces on the system, and $h_x(q, p), h_s(q, p)$ for the centrifugal, Coriolis and gravity terms. m_{xx} , m_{xs} , m_{sx} and m_{ss} represent the components of the $n \times n$ inertia matrix, and $B(q) \in \mathbb{R}^{m \times m}$ denotes input matrix which is of full rank.

In this paper, we will consider the control problem of the most difficult class of UMSs in their control design which are called Class-IIb UMSs. The following properties are distinguished this class of UMSs:

Assumption 1: The shape variables q_s are unactuated.

Assumption 2: There exists kinetic symmetry w.r.t external variables q_x .

Assumption 3. \dot{q}_x does not appear in the centrifugal, Coriolis and gravity terms, i.e. h_x and h_s .

This class has a nontriangular normal form which has attracted attentions particularly due to its application in tracking control of flexible-link manipulators.

For this class of UMSs, there exists a noncollocated partially linearizing invertible change of the control input τ as follows [1]

$$\tau = \alpha(q)u + \beta(q, \dot{q})$$

$$= (B^T B)^{-1} B^T \left[\left(m_{xx}(q_s) - m_{xs}(q_s) m_{ss}^{-1}(q_s) m_{sx}(q_s) \right) u + \left(h_x(q, \dot{q}) - m_{xs}(q_s) m_{ss}^{-1}(q_s) h_s(q, \dot{q}) \right) \right]$$
(2)

which transforms the dynamics of the Lagrangian model of Eq. 1 into a cascade combination of two reduced order nonlinear systems in the following form

$$\dot{q}_s = p_s
\dot{p}_s = f(q, p) + g(q)u
\dot{q}_x = p_x
\dot{p}_x = u$$
(3)

where, $f(q, p) : \mathbb{R}^{2n} \to \mathbb{R}^{n-m}$, $g(q) \in \mathbb{R}^{(n-m)\times m}$ are as follows

$$f(q, p) = -m_{ss}^{-1}(q)h_s(q, p)$$

$$g(q) = -m_{ss}^{-1}(q)m_{sx}(q)$$
(4)

Now, we can express the state vector X as X = $\begin{bmatrix} q_s & p_s & q_x & p_x \end{bmatrix}^T \in \mathbb{R}^{2n}$. The control objective is to design block backstepping algorithm for the trajectory tracking of the UMS shown in Eq. 3 such that the closed loop stability and asymptotic tracking are achieved.

3 Block Backstepping Control for the Class of UMSs

In this section, we present the design procedure of the block backstepping control method for the class of n-DOF UMS described in Section 2. We first devise the control algorithm to address the tracking control problem of the n-DOF UMS and then the stability of the proposed control approach is analysed.

3.1 The Controller Design

Since the Lagrangian model of the UMS under consideration in Eq. 1 is not in strict-feedback form and it may contain nonlinear coupling terms, so the integrator backstepping control algorithm is not directly applicable [11]. Therefore, we first transform the model of the UMS in Eq. 1 into a reduced order model with block-strict feedback form. Afterwards, the expression of the control input u is obtainable such that the reduced order system can track the desired trajectory.

The detailed procedure of designing the block backstepping approach is described in the following five steps:

Step 1: We consider the desired trajectory as:

$$X_d = \left[\begin{array}{ccc} q_{sd} & p_{sd} & q_{xd} & p_{xd} \end{array} \right]^T \tag{5}$$

The desired trajectory can be substituted in Eq. 3 in the following form:

$$\dot{q}_{sd} = p_{sd}
\dot{p}_{sd} = f(q_d, p_d) + g(q_d)u_d
\dot{q}_{xd} = p_{xd}
\dot{p}_{xd} = u_d$$
(6)

So the tracking errors can be defined as follows:

$$e = X - X_d = \begin{bmatrix} e_1 & e_2 & e_3 & e_4 \end{bmatrix}^T$$
 (7)

By differentiating both sides of Eq. 7, we have:

By differentiating both sides of Eq. 7, we have:

$$\begin{cases}
\dot{e}_1 = e_2 \\
\dot{e}_2 = (f(q, p) + g(q)u) - (f(q_d, p_d) + g(q_d)u_d) \\
\dot{e}_3 = e_4 \\
\dot{e}_4 = u - u_d
\end{cases}$$
(8)

Step 2: We define the following new control variable $z_1 \in$ \mathbb{R}^m by inspiring from [13] as:

$$z_1 = e_3 - K(e_1 + e_2 - ge_4) (9)$$

where $K \in \mathbb{R}^{m \times (n-m)}$ is a positive gain matrix with $K_{ij} = k$ when i = j, otherwise $K_{ij} = 0$. In Eq. 9, we denoted g(q) by g. Henceforth, for concise, we will show f(q, p), g(q), $f(q_d, p_d)$, $g(q_d)$ by f, g, f_d , g_d , respectively.



The dynamics of z_1 is derivable by differentiating both sides of Eq. 9 as follows

$$\dot{z}_1 = e_4 - K(e_2 + (f + gu) - (f_d + g_d u_d)
-gu - D(g)e_4)
= e_4 - K\Omega$$
(10)

where $\Omega = e_2 + f - f_d - g_d u_d - D(g) e_4$. In Eq. 10, $D(g) \in \mathbb{R}^{(n-m)\times m}$ denotes the time derivative of matrix g(q). The elements of D(g) can be expressed as $D(g_{ij}) = \sum_{k=1}^{n} \left(\partial g_{ij} / \partial q_k \right) p_k$.

Step 3: We define integral error variable as:

$$\chi_1 = \int_0^t z_1 dt \tag{11}$$

Then we can choose the following virtual control to stabilize z_1 subsystem:

$$\alpha_1 = -c_1 z_1 - \lambda \chi_1 + K\Omega \tag{12}$$

where λ and c_1 are arbitrary positive gains which should be designed. Considering the integral action in Eq. 12 may improve the tracking control performance

Step 4: We define the second control variable $z_2 \in \mathbb{R}^m$ as:

$$z_2 = e_4 - \alpha_1 \tag{13}$$

By substituting Eqs. 12 and 13 into Eq. 10, the dynamics of first control variable becomes:

$$\dot{z}_1 = z_2 - c_1 z_1 - \lambda \chi_1 \tag{14}$$

Consequently, by differentiating both sides of Eq. 13, the dynamics of the second control variable z_2 is obtainable as:

$$\dot{z}_{2} = \dot{e}_{4} - \dot{\alpha}_{1}
= u - u_{d} + c_{1}\dot{z}_{1} + \lambda\dot{\chi}_{1} - K\dot{\Omega}
= u - u_{d} + c_{1}\dot{z}_{1} + \lambda\dot{\chi}_{1}
- K \left(\frac{\partial\Omega}{\partial e_{1}}\dot{e}_{1} + \frac{\partial\Omega}{\partial e_{2}}\dot{e}_{2} + \frac{\partial\Omega}{\partial e_{3}}\dot{e}_{3} + \frac{\partial\Omega}{\partial e_{4}}\dot{e}_{4} \right)
+ \frac{\partial\Omega}{\partial q_{sd}}\dot{q}_{sd} + \frac{\partial\Omega}{\partial p_{sd}}\dot{p}_{sd} + \frac{\partial\Omega}{\partial q_{sd}}\dot{q}_{sd} + \frac{\partial\Omega}{\partial p_{sd}}\dot{p}_{sd} \right) (15)$$

where the expressions of the partial derivatives of vector Ω with respect to different sub-components of error vector and the desired trajectory vector can be written as

$$\begin{cases} \frac{\partial \Omega}{\partial e_1} = -\frac{\partial \left[m_{ss}^{-1}(e_1 + q_{sd})h_s(e + q_d, \dot{e} + \dot{q}_d)\right]}{\partial e_1} - \frac{\partial \left[D(g(e + q_d))\right]}{\partial e_1} e_4 \\ \frac{\partial \Omega}{\partial e_2} = 1 - \frac{\partial \left[m_{ss}^{-1}(e_1 + q_{sd})h_s(e + q_d, \dot{e} + \dot{q}_d)\right]}{\partial e_2} - \frac{\partial \left[D(g(e + q_d))\right]}{\partial e_2} e_4 \\ \frac{\partial \Omega}{\partial e_3} = -\frac{\partial \left[m_{ss}^{-1}(e_1 + q_{sd})h_s(e + q_d, \dot{e} + \dot{q}_d)\right]}{\partial e_3} - \frac{\partial \left[D(g(e + q_d))\right]}{\partial e_3} e_4 \\ \frac{\partial \Omega}{\partial e_4} = -\frac{\partial \left[m_{ss}^{-1}(e_1 + q_{sd})h_s(e + q_d, \dot{e} + \dot{q}_d)\right]}{\partial e_4} - \frac{\partial \left[D(g(e + q_d))\right]}{\partial e_4} e_4 - D(g) \end{cases}$$

and

$$\begin{cases} \frac{\partial \Omega}{\partial q_{sd}} = -\frac{\partial \left[m_{ss}^{-1}(e_1 + q_{sd}) h_s(e + q_d, \dot{e} + p_d) \right]}{\partial q_{sd}} + \frac{\partial \left[m_{ss}^{-1}(q_{sd}) h_s(q_d, p_d) \right]}{\partial q_{sd}} \\ + \frac{\partial \left[m_{ss}^{-1}(q_{sd}) m_{sx}(q_d) \right]}{\partial q_{sd}} u_d - \frac{\partial \left[D(g(e + q_d)) \right]}{\partial q_{sd}} e_4 \\ \frac{\partial \Omega}{\partial p_{sd}} = -\frac{\partial \left[h_s(e + q_d, \dot{e} + p_d) \right]}{\partial p_{sd}} m_{ss}^{-1}(e_1 + q_{sd}) + \frac{\partial \left[h_s(q_d, p_d) \right]}{\partial p_{sd}} m_{ss}^{-1}(q_{sd}) \\ \frac{\partial \Omega}{\partial q_{sd}} = -\frac{\partial \left[h_s(e + q_d, \dot{e} + p_d) \right]}{\partial q_{sd}} m_{ss}^{-1}(e_1 + q_{sd}) + \frac{\partial \left[h_s(q_d, p_d) \right]}{\partial q_{sd}} m_{ss}^{-1}(q_{sd}) \\ + \frac{\partial \left[m_{ss}(q_d) \right]}{\partial q_{sd}} m_{ss}^{-1}(q_{sd}) u_d - \frac{\partial \left[D(g(e + q_d)) \right]}{\partial q_{sd}} e_4 \\ \frac{\partial \Omega}{\partial p_{sd}} = -\frac{\partial \left[h_s(e + q_d, \dot{e} + p_d) \right]}{\partial p_{sd}} m_{ss}^{-1}(e_1 + q_{sd}) + \frac{\partial \left[h_s(q_d, p_d) \right]}{\partial p_{sd}} m_{ss}^{-1}(q_{sd}) \end{cases}$$

$$(17)$$

Therefore the dynamics of the second control variable becomes

$$\dot{z}_2 = u - u_d + c_1 (z_2 - c_1 z_1 - \lambda \chi_1) + \lambda z_1 - K \dot{\Omega}$$
(18)

In the steps above the cascade nonlinear form of n-DOF UMS of Eq. 3 was transformed into the block-strict feedback form.

Step 5: The desired dynamics for z_2 can be written as:

$$\dot{z}_2 = -z_1 - c_2 z_2 \tag{19}$$

where c_2 is an arbitrary positive gain which should be designed.

Eventually, the control law u is designable to establish the desired dynamics in Eq. 19. By combining Eqs. 18 and 19, we obtain the control law u for the UMS as follows:

$$u = -(1 - c_1^2 + \lambda)z_1 - (c_1 + c_2)z_2 + \lambda c_1 \chi_1 + u_d + K\dot{\Omega}$$
 (20)

Now, by substituting the above control law Eq. 20 into Eq. 18, the following error dynamics is resulted

$$\begin{cases} \dot{z}_1 = z_2 - c_1 z_1 - \lambda \chi_1 \\ \dot{z}_2 = -z_1 - c_2 z_2 \end{cases}$$
 (21)

3.2 Stability and Convergence Analysis

Theorem 1 By applying the control law of Eq. 20 for the UMS under dynamics of Eq. 1, the trajectory tracking onto continuous desired trajectories is achievable which are differentiable of order 2 with respect to time.

Proof To this end, we prove that the closed-loop system obtained in Eq. 21 is asymptotically stable and the trajectory tracking is achievable by employing the control law u in Eq. 20.

We define a candidate for Lyapunov function as:

$$V = \frac{1}{2}\lambda\chi_1^2 + \frac{1}{2}z_1^2 + \frac{1}{2}z_2^2$$
 (22)



By differentiating both sides of Eq. 22 and substituting by Eq. 21, we obtain:

$$\dot{V} = \lambda \chi_1 \dot{\chi}_1 + z_1 \dot{z}_1 + z_2 \dot{z}_2
= \lambda \chi_1 z_1 + z_1 (z_2 - c_1 z_1 - \lambda \chi_1) + z_2 (-z_1 - c_2 z_2)
= -c_1 z_1^2 - c_2 z_2^2 \le 0$$
(23)

The inequality $\dot{V} \leq 0$ resulted in Eq. 23 implies the fact that V(t) < V(0), thus, χ_1, z_1 , and z_2 all are bounded together with \dot{z}_1 and \dot{z}_2 , since the expressions in Eq. 21 are fulfilled.

The second time-derivative of V is obtainable as:

$$\ddot{V} = -2c_1z_1\dot{z}_1 - 2c_2z_2\dot{z}_2\tag{24}$$

Since z_1 , z_2 , \dot{z}_1 , and \dot{z}_2 all are bounded, Eq. 24 implies that \dot{V} is bounded, too. Therefore, the convergence of z_1 and z_2 to zero is achieved as $t \to \infty$ according to Barbalat Lemma [10].

Theorem 2 By applying the control law in Eq. 20 and considering the initial conditions $X(0) = [q_s(0) \ p_s(0) \ q_x(0) \ p_x(0)]^T$, the trajectory tracking errors in Eq. 7 asymptotically converge to zero in a finite time.

Proof Since the convergence of z_1 to zero point has been proved and K is a positive gain, Eq. 9 yields:

$$\lim_{t \to \infty} e_3 = \lim_{t \to \infty} [K(e_1 + e_2 - ge_4)] = 0$$
 (25)

By convergence of z_2 to zero and considering Eqs. 12 and 13, one can conclude that:

$$\lim_{t \to \infty} e_4 = \lim_{t \to \infty} \alpha_1 = \lim_{t \to \infty} \Omega = 0$$
 (26)

Therefore, Eqs. 25 and 26 result in:

$$\lim_{t \to \infty} e_1 = \lim_{t \to \infty} e_2 = 0 \tag{27}$$

Hence, the four components of the tracking errors in Eq. 7 asymptotically converge to zero.

4 Dynamics of the SFLFJM

The schematic diagram of the planar SFLFJM with coordinate system is given in Fig. 1. It consists a link of length L, Young modules E, mass per unit length ρ and second moment of area I, a joint with flexibility k_{jo} , an actuator with a hub mass of m_h and hub mass moment of inertia of I_h , and a rotor mass of m_r and rotor mass moment of inertia of I_r . Since the actuator of the link is attached to the ground, m_h , I_h and m_r do not affect the dynamics [18]. Finally, the mass and mass moment of inertia for the payload are represented by m_{tip} and I_{tip} , respectively.

Dynamics of the planar SFLFJM is presentable as follows [18].

$$M\ddot{q} + C\dot{q} + Kq + G = B\tau \tag{28}$$

where $q = \begin{bmatrix} q_J & q_L \\ \theta_J & \theta_L & \delta_1 & \delta_2 \end{bmatrix}^T$ includes the first two mode

shapes, δ_1 and δ_2 are flexible modes or mode amplitudes, q_J is the vector of states related to the joint and q_L is the vector of states related to the link, $B = \begin{bmatrix} 1 & 0 & 0 & 0 \end{bmatrix}^T$, τ is the torque of the actuator and M, C, K and G are given in Appendix. For SFLFJM, we have $B \in \mathbb{R}^{4 \times 1}$ with m = rank(B) = 1, which is not of full rank n = 4 (m < n), therefore the underactuation degree is n - m = 3.

We define the tip position for the SFLFJM as

$$y(L,t) = L\theta_J(t) + L\theta_L(t) + \xi(L,t)$$
(29)

where

$$\xi(L,t) = \phi_1(L)\delta_1(t) + \phi_2(L)\delta_2(t)$$
(30)

stands for tip deflection of the flexible-link.

We consider the following output q_r by dividing both sides of Eq. 29 by L as follows

$$q_r = \theta_J + \theta_L + \frac{1}{I} (\phi_1(L)\delta_1 + \phi_2(L)\delta_2)$$
 (31)

The first and the second time derivatives of Eq. 31 yield

$$\dot{q}_r = \dot{\theta}_J + \dot{\theta}_L + \frac{1}{L} \left(\phi_1(L) \dot{\delta}_1 + \phi_2(L) \dot{\delta}_2 \right) \tag{32}$$

$$\ddot{q}_r = \ddot{\theta}_J + \ddot{\theta}_L + \frac{1}{L} \left(\phi_1(L) \ddot{\delta}_1 + \phi_2(L) \ddot{\delta}_2 \right) \tag{33}$$

We can rewrite Eq. 28 in the following form

$$\begin{bmatrix} M_{rr} & 0 \\ 0 & M_{ff} \end{bmatrix} \begin{bmatrix} \ddot{q}_J \\ \ddot{q}_L \end{bmatrix} + \begin{bmatrix} 0 & 0 \\ 0 & C_{ff} \end{bmatrix} \begin{bmatrix} \dot{q}_J \\ \dot{q}_L \end{bmatrix} + \begin{bmatrix} K_{rr} & K_{rf} \\ K_{fr} & K_{ff} \end{bmatrix} \begin{bmatrix} q_J \\ q_L \end{bmatrix} + \begin{bmatrix} G_r \\ G_f \end{bmatrix} = \begin{bmatrix} 1 \\ 0 \end{bmatrix} \tau$$
(34)

where subscriptions r and f refer to rigid and flexible deformations, respectively.

By defining the new coordinates $\bar{q} = [q_r \quad q_L]^T$, the dynamics of the planar SFLFJM in horizontal plane (G = 0) is obtainable by Eq. 34 in the new coordinates as:

$$\bar{M}\ddot{\bar{q}} + \bar{C}\dot{\bar{q}} + \bar{K}\bar{q} = B\tau \tag{35}$$

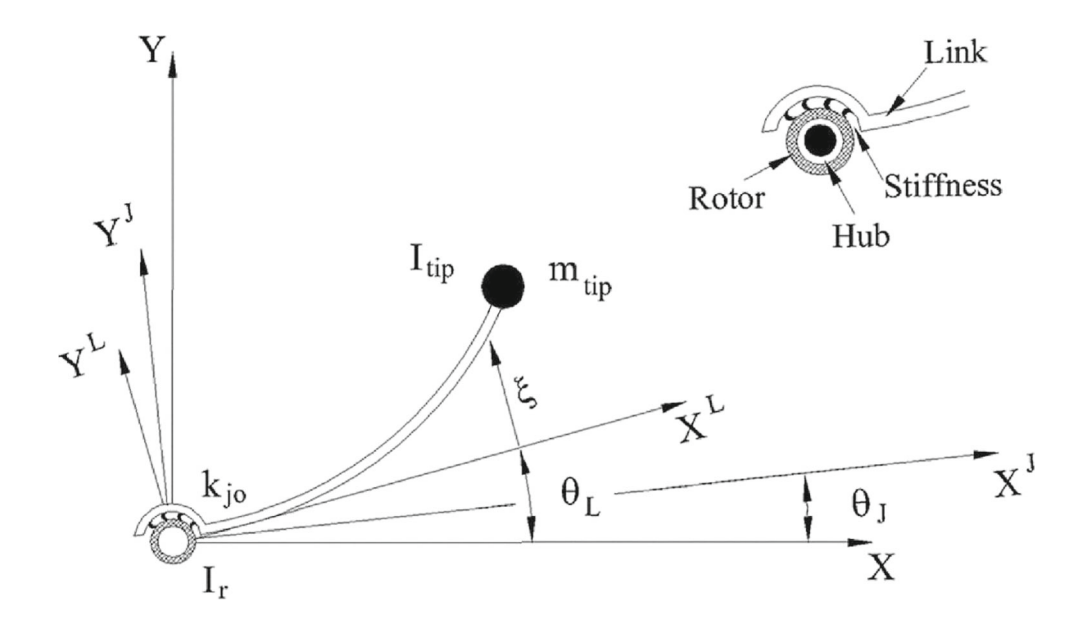
where the new mass, damping and stiffness matrices are obtainable as follows.

$$\bar{M} = \begin{bmatrix} M_{rr} - M_{rr} \Phi \\ 0 & M_{ff} \end{bmatrix} \tag{36}$$

$$\bar{C} = \begin{bmatrix} 0 & 0 \\ 0 & C_{ff} \end{bmatrix} \tag{37}$$

$$\bar{K} = \begin{bmatrix} K_{rr} & (K_{rf} - K_{rr}\Phi) \\ K_{fr} & (K_{ff} - K_{fr}\Phi) \end{bmatrix}$$
(38)

Fig. 1 Schematic of the planar SFLFJM



$$B = \begin{bmatrix} 1 \\ 0_{31} \end{bmatrix} \tag{39}$$

where $\Phi = \begin{bmatrix} 1 & \phi_1/L & \phi_2/L \end{bmatrix}$.

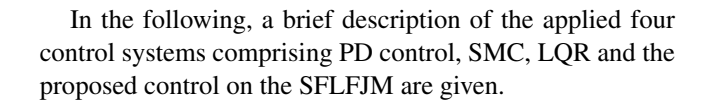
Now, we can define the conjugate momentum in the new coordinates as:

$$p = \bar{M}\,\dot{\bar{q}}\tag{40}$$

5 Simulation Results

In this section, the proposed control system compared with some related control systems are applied to control the SFLFJM as a case study for the UMSs. To this end, through simulation tests carried out by using MATLAB software, the effectiveness and performance of the proposed controller is investigated.

We employ the model of the flexible-link flexible-joint manipulator presented in [18] whose parameter values are listed in Table 1. Also, we use a quasi-static tracking error system along desired trajectory of the end-point of the SFLFJM as $q_d = \left[\pi/2 \, \pi/4 \, 0 \, 0\right]^T$, with $\dot{q}_d = \ddot{q}_d = 0$ and $p_d = \dot{p}_d = 0$. The objective is to track the trajectory of the end-effector of the SFLFJM to the desired position with vibration suppression. To this purpose, the initial state vector is selected as $x(0) = \left[e(0) \, p_e(0)\right]^T = \left[\pi/2 \, \pi/4 \, 0_{1\times 6}\right]^T$ in accordance with the defined desired trajectory.



5.1 PD Control

First, the following PD control law like that proposed in [19] is imposed to the SFLFJM.

$$u = k_p x_e + k_d \dot{x}_e \tag{41}$$

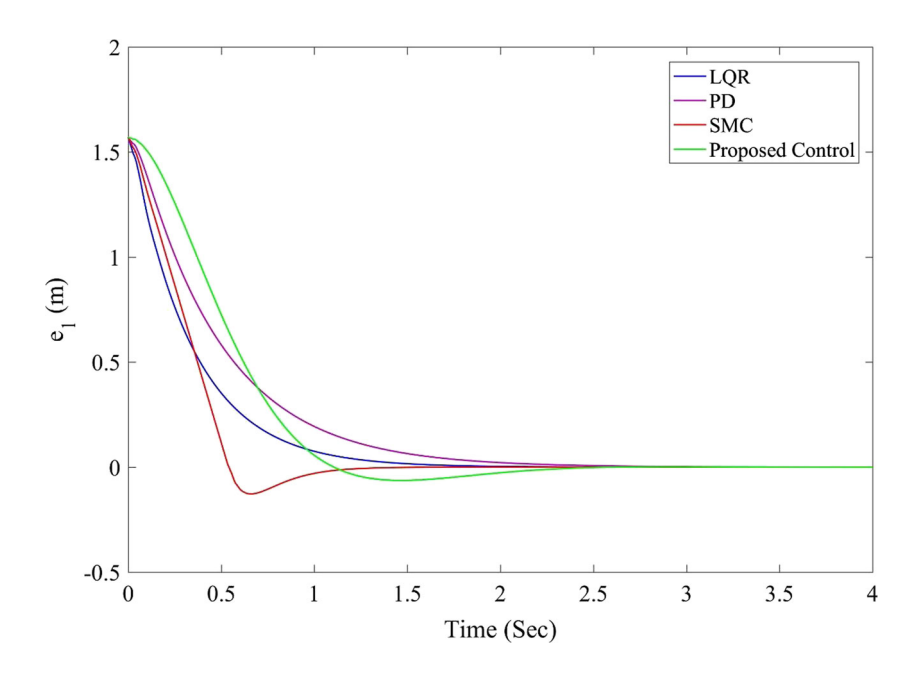
The PD gains applied in our simulation study are set as: $k_p = \begin{bmatrix} 0.2 & 0.16 & 0.08 & 0.05 \end{bmatrix}$ and $k_d = \begin{bmatrix} 0.25 & 0.20 & 0.12 & 0.08 \end{bmatrix}$.

 $\begin{tabular}{ll} \textbf{Table 1} & Physical parameters of the SFLFJM used for the simulation study $[18]$ \\ \end{tabular}$

Physical parameters	Value
L (Length of the link)	0.3 (m)
E (Young's modulus of the link)	20 (GPa)
I (Second moment of area of the link)	$833.3 \times 10^{-12} (\text{m}^4)$
ρ (Mass per unit length of the link)	0.0549 (kg/m)
I_h (Mass moment of inertia of the link)	$1.2 \times 10^{-4} (\text{kg.m}^2)$
I_r (Mass moment of inertia of rotor at the joint)	$1.2 \times 10^{-6} (\text{kg.m}^2)$
k_{jo} (Spring stiffness at the joint)	100 (N.m/rad)
h (Gear ratio at the joint)	10
m_{tip} (Mass of the payload)	0.19 (kg)
I_{tip} (Mass moment of inertia of the payload)	$0.01 (kg.m^2)$



Fig. 2 The tracking error of q_r through LQR, PD, SMC and proposed control systems



5.2 Conventional Sliding Mode Control with PD Sliding Surface

The second simulated controller for the SFLFJM is a conventional SMC with a PD sliding surface similar to that proposed by [20]:

$$s(t) = \dot{x}_e - Cx_e \tag{42}$$

where, $C = \text{diag}(c_1, c_2, c_3, ..., c_8)$ with $c_i > 0$. The system will operate in the sliding mode while satisfying: s(t) = 0 and $\dot{s}(t) = 0$.

In order to get a suitable sliding surface, we must design the SMC in such a way that it can drive the states of the SFLFJM into the sliding surface s(t) = 0. We obtain the SMC law as:

$$u_c = (Cg)^{-1}C[(J-R)(\nabla_{x_e}H_e)^T] - \eta \text{sat}(s/\mu)$$
 (43)

where $\eta > 0$, and the saturation function, $\operatorname{sat}(s/\mu)$ is a replacement for the discontinuous term $\operatorname{sgn}(s)$. In our simulations, we set the values of these parameters as: $\eta = 300$, $\mu = 0.02$, $C = \operatorname{diag}([10\ 10\ 1.5\ 1.5\ 2\ 2\ 2\ 2])$.

5.3 Linear Quadratic Regulator (LQR)

In order to design the well-known LQR controller, a linear state space dynamic model of the SFLFJM should be

Fig. 3 The tracking error of θ_L through LQR, PD, SMC and proposed control systems

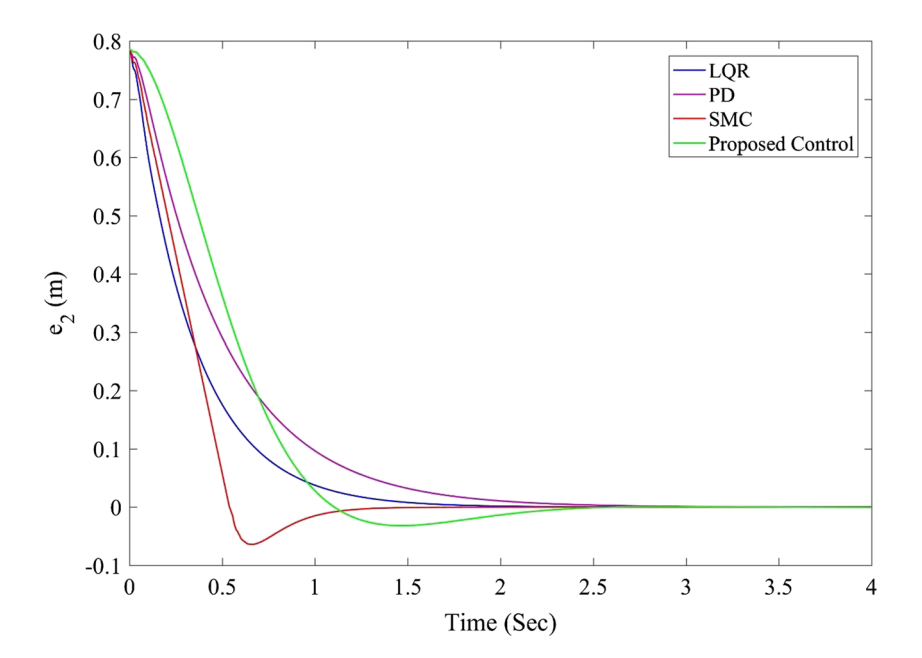
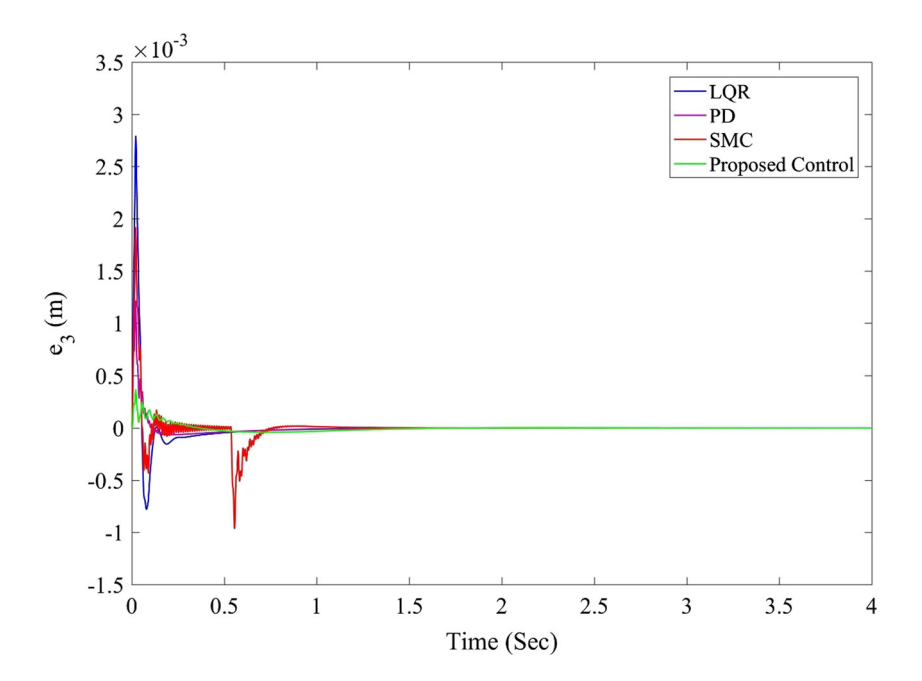




Fig. 4 The tracking error of δ_1 through LQR, PD, SMC and proposed control systems



obtained by linearization of the equations of motion of the system in Eq. 35. We consider the tracking errors, $x_e = x - x_d$ as our states in which,

$$x = \left[q_r \ \dot{q}_r \ \theta_L \ \dot{\theta}_L \ \delta_1 \ \dot{\delta}_1 \ \delta_2 \ \dot{\delta}_2 \right]^T \tag{44}$$

and

$$x_d = \left[\pi/2 \ 0 \ \pi/4 \ 0 \ 0 \ 0 \ 0 \right]^T \tag{45}$$

(46)

By linearizing Eq. 35, we obtain the LTI system as

$$\dot{x}_e = Ax_e + Bu$$

with A and B being as:

Fig. 5 The tracking error of δ_2 through LQR, PD, SMC and proposed control systems

$$A = \begin{bmatrix} 0 & 1 & 0 & 0 & 0 & 0 & 0 & 0 \\ -832825.4 & 0 & 1665650.8 & 0 & 5471327.5 & 0 & -6498914.9 & 0 \\ 0 & 0 & 0 & 1 & 0 & 0 & 0 & 0 \\ 47803.9 & 0 & -95607.9 & 0 & 279071.5 & 0 & 2528899.4 & 0 \\ 0 & 0 & 0 & 0 & 0 & 1 & 0 & 0 & 0 \\ -7832.2 & 0 & 15664.4 & 0 & -65394.8 & 0 & -673431.3 & 0 \\ 0 & 0 & 0 & 0 & 0 & 0 & 0 & 1 \\ -737 & 0 & 1474.1 & 0 & -10896 & 0 & -153211.6 & 0 \end{bmatrix},$$

$$B = \begin{bmatrix} 0 \\ 8333.3 \\ 0 \\ 0 \\ 0 \\ 0 \\ 0 \\ 0 \end{bmatrix} \tag{47}$$

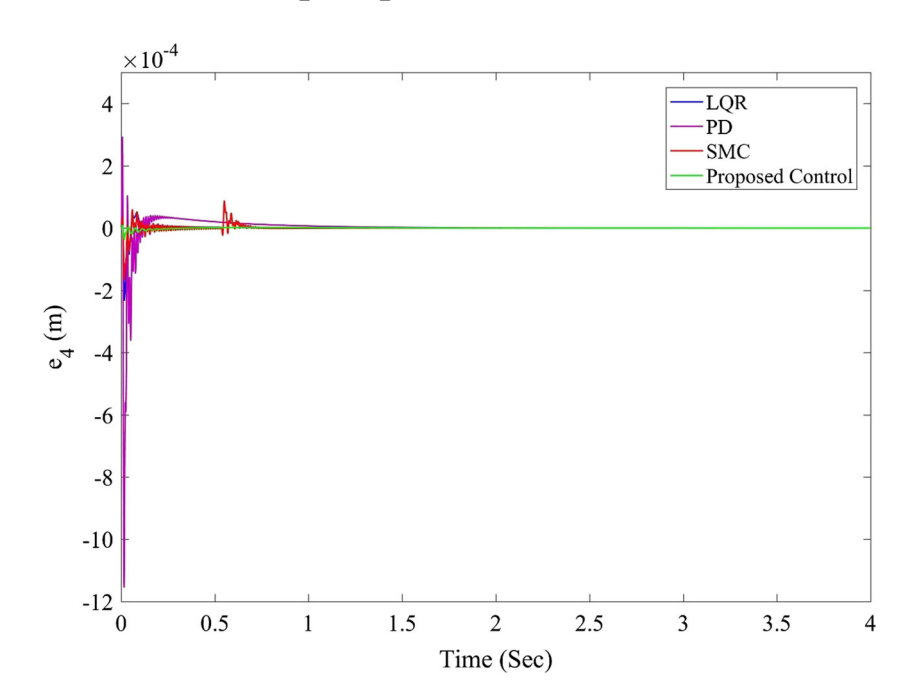
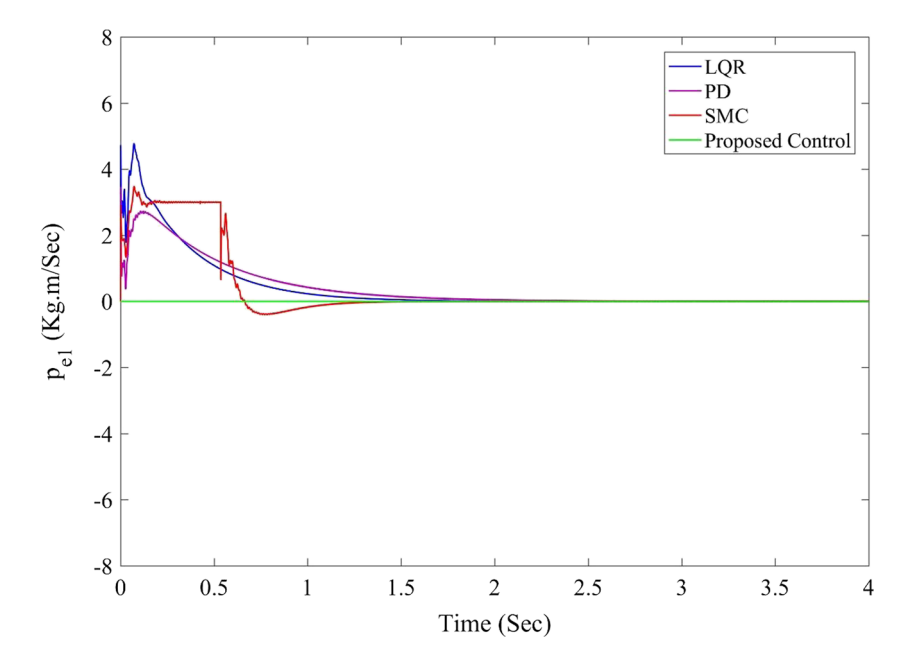




Fig. 6 The momentum error of p_{e1} through LQR, PD, SMC and proposed control systems



The LQR control system is simulated based on the following cost function and design weighting matrices therein.

$$J = \int_0^\infty (x^T Q x + u^T R u) dt \tag{48}$$

$$Q = \text{diag} ([1 \ 0.1 \ 0.5 \ 0.05 \ 100 \ 2 \ 2000 \ 20])$$
 $R = 0.1$ (49)

The LQR control law is applied as

$$u = -Kx_e$$

$$K = R^{-1}B^TX$$

Fig. 7 The momentum error of p_{e2} through LQR, PD, SMC and proposed control systems

where X is the solution of the following algebraic Riccati equation

$$A^{T}X + XA - XBR^{-1}B^{T}X + Q = 0 (51)$$

For the aforementioned system in Eq. 46, the LQR gain matrix is computed as

$$K = \begin{bmatrix} 106.1 & 1.013 & -205.45 & 0.1959 & 604.7 & -0.5164 & 5999.7 & -0.4846 \end{bmatrix}$$
 (52)

5.4 The Proposed Block-Backstepping Approach

In this subsection, we consider the SFLFJM in Eq. 35 as an (50) UMS which its dynamics was shown in Eq. 1 with $q_x =$

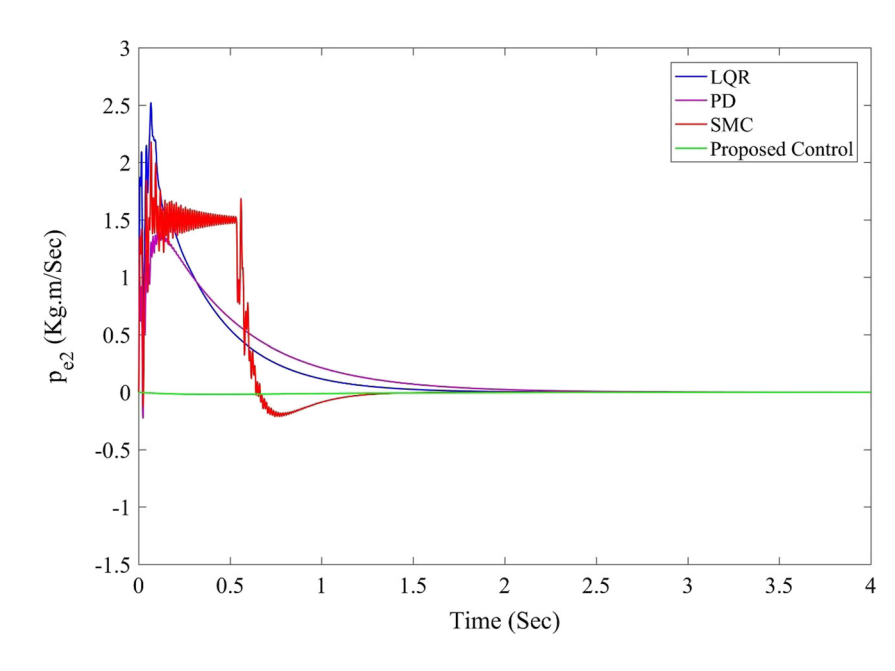
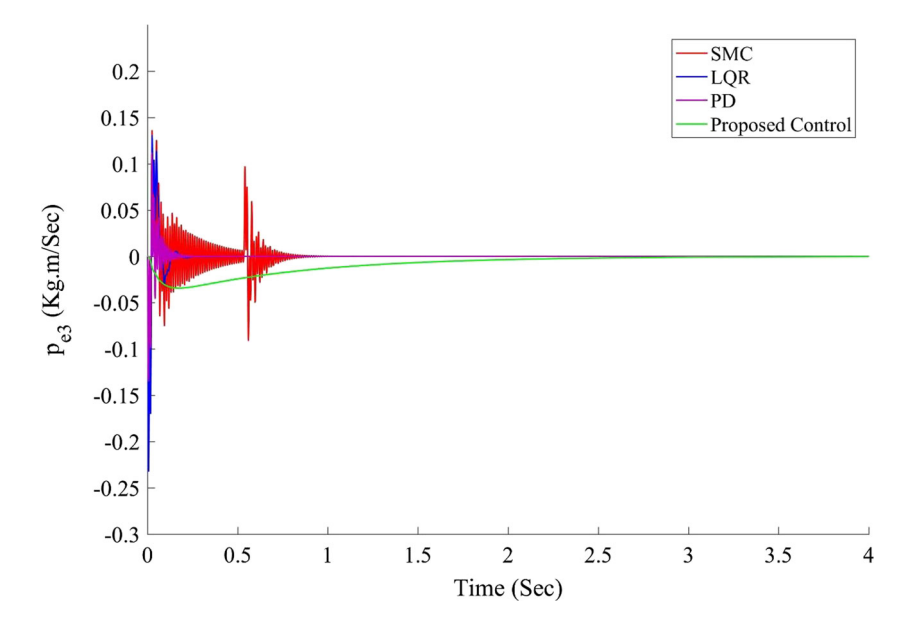




Fig. 8 The momentum error of p_{e3} through LQR, PD, SMC and proposed control systems



 $[\ q_r\ q_L]^T$ and $q_s=[\ \delta_1\ \delta_2]^T$. Hence, the state vector can be expressed as

$$X = \begin{bmatrix} \delta_1 & \delta_2 & \dot{\delta}_1 & \dot{\delta}_2 & q_r & q_L & \dot{q}_r & \dot{q}_L \end{bmatrix}^T$$
 (53)

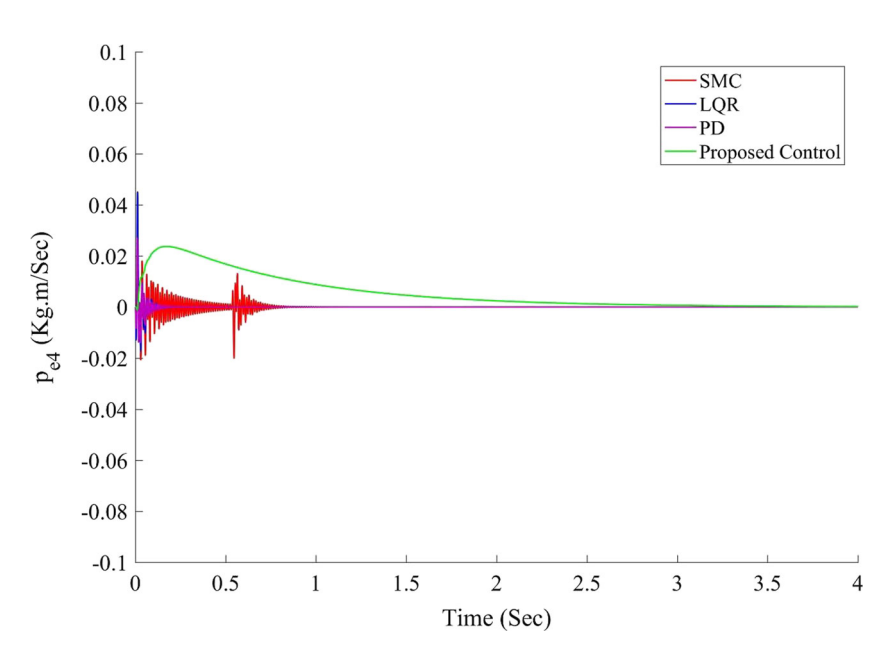
Now, z_1 is defined as

$$z_1 = e_3 - K(e_1 + e_2 - ge_4) (54)$$

where $e_1 = q_s - q_{sd}$, $e_2 = \dot{q}_s - \dot{q}_{sd}$, $e_3 = q_x - q_{xd}$, and $e_4 = \dot{q}_x - \dot{q}_{xd}$. The matrix K is a diagonal matrix as $K = \text{diag}\{k, k\}$. For the defined regulation problem of the SFLFJM in this section, the desired control input is zero, i.e. $u_d = 0$. Therefore, the control input u is resulted according to Eq. 20 as follows

$$u = -(1 - c_1^2 + \lambda)z_1 - (c_1 + c_2)z_2 + \lambda c_1 \chi_1 + K\dot{\Omega}$$
 (55)

Fig. 9 The momentum error of p_{e4} through LQR, PD, SMC and proposed control systems



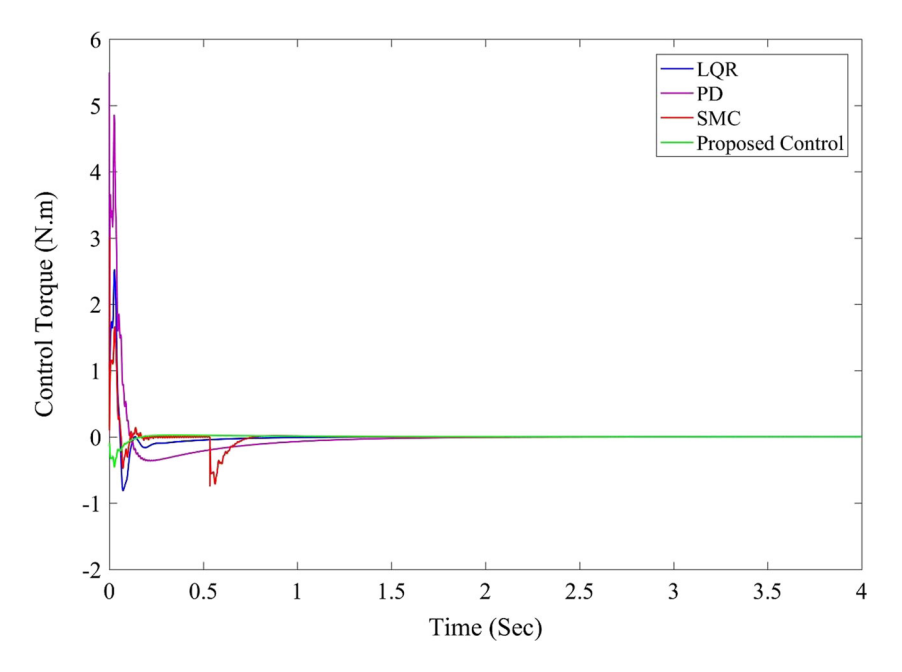
Then, the control torque τ required to drive the SFLFJM in Eq. 35 is computed using Eq. 2. The control design parameters c_1 , c_2 , λ , and k should be chosen such that the conditions c_1 , c_2 , k, $\lambda > 0$ are satisfied. The control parameters values are chosen as $c_1 = 300$, $c_2 = 0.9$, k = 10, and $\lambda = 0.3$.

Now, the simulation results for the tracking errors and resultant momentum errors ($p_e = \bar{M}\dot{e}$) of the three LQR, PD and conventional SMC control systems are compared with respect to the proposed block backstepping control in Figs. 2, 3, 4, 5, 6, 7, 8, 9 and 10.

In Figs. 2–10, the simulation results show the superiority of the proposed control method compared with the LQR, PD controller, and the conventional SMC. The dynamic responses of the SFLFJM for the tracking errors of the tip



Fig. 10 The control torque τ of LQR, PD, SMC and proposed control systems



position and the first two flexible modes in horizontal plane are shown in Figs. 2–5. Figures 6–9 show the simulation results for the resultant momentum errors corresponding to the four tracking errors whereas all the tracking errors and the resultant momentum errors converge to zero, i.e. to the equilibrium point, $x_e = 0$ without any residual vibrations. Furthermore, the applied control torques by the application of the four control systems are depicted in Fig. 10. It is observable from the results of the four controllers, under the proposed controller the SFLFJM is moving faster to its desired tip position and the vibrations are alleviated in a faster manner. From the torque results, it can be seen that the variations of the control torque applied to the system are in a practically applicable range. Hence, the simulation results show that the proposed block backstepping approach has an excellent performance and a very rapidly convergence to the desired trajectory during the motion control of the SFLFJM. From the simulation tests, we found that although higher control torques can cause faster convergence to the desired trajectory, however, they may also lead to residual vibrations, concurrently.

6 Conclusions

In this paper, a novel trajectory tracking control was proposed for the upmost general class of UMSs called as Class-II UMSs from the control point of view. The reduced-order block backstepping method was used to address the tracking and stabilization problems associated with the UMSs with nontriangular normal form. The designed control system can ensure the global asymptotic stability

and convergence of the UMSs according to the Lyapunov theory and Barbalat Lemma. The proposed algorithm was employed to address the end-effector trajectory tracking of the SFLFJM in horizontal plane as a case study for Class-IIb UMSs to demonstrate the performance of the control scheme. The simulation results of the proposed control system were compared with three conventional controllers comprising LQR, PD, and SMC and thus verified the superiority of the proposed control scheme in terms of fast converging and low tracking errors.

Appendix: Dynamic Model of the SFLFJM

Mass matrix:

$$M = M_{FI} + M_{FR}$$

where

where

$$\begin{split} M_{11} &= (\rho L^3)/3 + \rho(\Phi_{11}\delta_1^2 + 2\Phi_{12}\delta_1\delta_2 + \Phi_{22}\delta_2^2) \\ &+ I_h + I_{tip} + m_{tip}L^2 + m_{tip}(\phi_1^2(L)\delta_1^2 \\ &+ 2\phi_1(L)\phi_2(L)\delta_1\delta_2 + \phi_2^2(L)\delta_2^2) \\ M_{12} &= \rho\Phi_{1x} + m_{tip}L\phi_1(L) + I_{tip}\phi_1'(L) \\ M_{21} &= M_{12} \end{split}$$



$$M_{13} = \rho \Phi_{2x} + m_{tip} L \phi_2(L) + I_{tip} \phi_2'(L)$$

$$M_{31} = M_{13}$$

$$M_{22} = \rho \Phi_{11} + m_{tin} \phi_1^2(L) + I_{tin} \phi_1'^2(L)$$

$$M_{23} = \rho \Phi_{11} + m_{tip}\phi_1(L)\phi_2(L) + I_{tip}\phi_1'(L)\phi_2'(L)$$

$$M_{32} = M_{23}$$

$$M_{33} = \rho \Phi_{22} + m_{tip} \phi_2^2(L) + I_{tip} \phi_2^{\prime 2}(L)$$

Stiffness matrix:

$$K = K_{FI} + K_{FR}$$

where

where

$$K_{11} = EI\Phi_{11xx}$$

$$K_{12} = EI\Phi_{12xx}$$

$$K_{21} = K_{12}$$

$$K_{22} = EI\Phi_{22xx}$$

Dissipation matrix:

$$C = \begin{bmatrix} 0 & 0 & 0 & 0 \\ 0 & C_{11} & C_{12} & C_{13} \\ 0 & C_{21} & C_{22} & C_{23} \\ 0 & C_{31} & C_{32} & C_{33} \end{bmatrix}$$

where

$$C_{11} = \rho(\dot{\delta}_{1}(\delta_{1}\Phi_{11} + \delta_{2}\Phi_{12}) + \dot{\delta}_{2}(\delta_{2}\Phi_{22} + \delta_{1}\Phi_{12})) + m_{tip}(\phi_{1}^{2}(L)\dot{\delta}_{1}\delta_{1} + \phi_{1}(L)\phi_{2}(L)\dot{\delta}_{1}\delta_{2} + \phi_{1}(L)\phi_{2}(L)\dot{\delta}_{2}\delta_{1} + \delta_{2}\dot{\delta}_{2}\phi_{2}^{2}(L));$$

$$C_{12} = \rho \dot{\theta}_L (\delta_1 \Phi_{11} + \delta_2 \Phi_{12}) + m_{tip} \dot{\theta}_L (\delta_1 \phi_1^2(L) + \phi_1(L)\phi_2(L)\delta_2);$$

$$C_{21} = -C_{12}$$

$$C_{13} = \rho \dot{\theta}_L (\delta_2 \Phi_{22} + \delta_1 \Phi_{12}) + m_{tip} \dot{\theta}_L (\delta_1 \phi_1(L) \phi_2(L) + \delta_2 \phi_2^2(L));$$

$$C_{31} = -C_{13}$$

$$C_{23} = 0$$

$$C_{32} = 0$$

$$C_{22} = 0$$

$$C_{33} = 0$$

Gravity vector:

$$G = \begin{bmatrix} G_1 \\ G_2 \\ G_3 \\ G_4 \end{bmatrix}$$



where

$$G_1 = 0;$$

$$G_2 = \rho g(L^2/2)cos(\theta_L) - \rho g(\delta_1 \Phi_{10} + \delta_2 \Phi_{20})sin(\theta_L);$$

$$G_3 = \rho g \Phi_{10} cos(\theta_L);$$

$$G_4 = \rho g \Phi_{20} cos(\theta_L);$$

where

$$\Phi_{10} = \int_0^L \phi_1(x) dx$$

$$\Phi_{20} = \int_0^L \phi_2(x) dx$$

$$\Phi_{11} = \int_0^L \phi_1^2(x) dx$$

$$\Phi_{12} = \int_0^L \phi_1(x) \phi_2(x) dx$$

$$\Phi_{22} = \int_0^L \phi_2^2(x) dx$$

$$\Phi_{1x} = \int_0^L x \phi_1(x) dx$$

$$\Phi_{2x} = \int_0^L x \phi_2(x) dx \Phi_{11xx} = \int_0^L \left(\frac{d^2 \phi_1(x)}{dx^2} \right)^2 dx$$

$$\Phi_{12xx} = \int_0^L \left(\frac{d^2\phi_1(x)}{dx^2}\right) \left(\frac{d^2\phi_2(x)}{dx^2}\right) dx$$

$$\Phi_{22xx} = \int_0^L \left(\frac{d^2 \phi_2(x)}{dx^2} \right)^2 dx$$

where

$$\phi_1(\mathbf{x}) = \cosh(\mu_1 \mathbf{x}) - \cos(\mu_1 \mathbf{x}) - \gamma_1(\sinh(\mu_1 \mathbf{x}) - \sin(\mu_1 \mathbf{x}))$$

$$\phi_2(x) = \cosh(\mu_2 x) - \cos(\mu_2 x) - \gamma_2(\sinh(\mu_2 x) - \sin(\mu_2 x))$$

where

$$\mu_1 = \frac{\beta_1}{L}, \mu_2 = \frac{\beta_2}{L}$$

 $\beta_1 = 1.8751, \beta_2 = 4.6941, \gamma_1 = 0.7341, \gamma_2 = 1.0185$

Publisher's Note Springer Nature remains neutral with regard to jurisdictional claims in published maps and institutional affiliations.

References

- Spong, M.W.: Underactuated mechanical systems. In: Control Problems in Robotics and Automation, pp. 135–150. Springer, Berlin (1998)
- 2. Liu, Y., Yu, H.: A survey of underactuated mechanical systems. IET Control Theor. Appl. **7**(7), 921–935 (2013)
- Olfati-Saber, R.: Nonlinear Control of Underactuated Mechanical Systems with Application to Robotics and Aerospace Vehicles. Massachusetts Institute of Technology (2001)
- Fantoni, I., Lozano, R.: Non-linear Control for Underactuated Mechanical Systems. Springer Science & Business Media, London (2002)

- Aneke, N.P.I.: Control of Underactuated Mechanical Systems. Technische Universiteit Eindhoven (2003)
- Maalouf, D., Moog, C.H., Aoustin, Y., Li, S.: Classification of two-degree-of-freedom underactuated mechanical systems. IET Control Theor. Appl. 9(10), 1501–1510 (2015)
- Zhang, M., Ma, X., Rong, X., Tian, X., Li, Y.: Error tracking control for underactuated overhead cranes against arbitrary initial payload swing angles. Mech. Syst. Signal Process. 84, 268–285 (2017)
- Sepulchre, R., Jankovic, M., Kokotovic, P.V.: Constructive Nonlinear Control. Springer Science & Business Media (2012)
- Kokotović, P., Arcak, M.: Constructive nonlinear control: a historical perspective. Automatica 37(5), 637–662 (2001)
- Khalil, H.K.: Noninear Systems, vol. 2, pp. 5–1. Prentice-Hall, New Jersey (1996)
- 11. Krstic, M., Kanellakopoulos, I., Kokotovic, P.V.: Nonlinear and Adaptive Control Design, vol. 222. Wiley, New York (1995)
- Chang, Y., Cheng, C.-C.: Block backstepping control of multiinput nonlinear systems with mismatched perturbations for asymptotic stability. Int. J. Control 83(10), 2028–2039 (2010)
- Rudra, S., Barai, R.K., Maitra, M.: Nonlinear state feedback controller design for underactuated mechanical system: a modified block backstepping approach. ISA Trans. 53(2), 317–326 (2014)
- Rudra, S., Barai, R.K., Maitra, M.: Block Backstepping Design of Nonlinear State Feedback Control Law for Underactuated Mechanical Systems. Springer, Berlin (2016)
- Chang, Y.: Block backstepping control of MIMO systems. IEEE Trans. Autom. Control 56(5), 1191–1197 (2011)
- Rudra, S., Barai, R.K., Maitra, M.: Design and implementation of a block-backstepping based tracking control for nonholonomic wheeled mobile robot. Int. J. Robust Nonlinear Control 26(14), 3018–3035 (2016)
- Dong, Z., Wan, L., Li, Y., Liu, T., Zhang, G.: Trajectory tracking control of underactuated USV based on modified backstepping approach. Int. J. Naval Archit. Ocean Eng. 7(5), 817–832 (2015)
- Vakil, M., Fotouhi, R., Nikiforuk, P.: A new method for dynamic modeling of flexible-link flexible-joint manipulators. J. Vib. Acoust. 134(1), 014503 (2012)
- Staufer, P., Gattringer, H., Bremer, H.: Comparative study on control concepts of a robot manipulator with multiple-link/joint flexibilities. PAMM 12(1), 79–80 (2012)

 Suklabaidya, S., Lochan, K., Roy, B.: Modeling and sliding mode control of flexible link flexible joint robot manipulator. In: Proceedings of the 2015 Conference on Advances in Robotics, p. 59. ACM (2015)

Mohammad-Reza Moghanni-Bavil-Olyaei received his B.Sc. and M.Sc. degrees both in Mechanical Engineering from University of Tabriz, Tabriz, Iran, in 2008 and 2011 respectively. He is currently a Ph.D. candidate in the Mechanical Engineering Department at University of Tabriz, Tabriz, Iran. His research interests include flexible manipulators, port-controlled Hamiltonian systems, nonlinear control methods and their applications in underactuated mechanical systems.

Ahmad Ghanbari received the B.Sc. and M.Sc. degrees in Mechanical Engineering from California Polytechnic State University, Pomona, California, in 1978 and 1980 respectively. He received his Ph.D. degree in electrical engineering from University of Tabriz, Tabriz, Iran in 2007. He is currently a professor with the School of Engineering Emerging Technologies at University of Tabriz. His research interests include mechatronics, dynamics, control, robotics, and artificial intelligence. He is author and coauthor of more than 100 journal and conference papers related to these fields. He is a member of ASME, Iranian Society of Mechanical Engineering (ISME) and Iranian Society of Mechatronics. Also, he is director of Center of Excellence for Mechatronics at the University of Tabriz.

Jafar Keighobadi received his B.Sc. degree in mechanical engineering from University of Tabriz, Tabriz, Iran, in 1997, and M.S. and Ph.D. degrees in mechanical engineering and control systems from Amirkabir University of Technology (Tehran Polytechnic), Tehran, Iran in 2000 and 2008, respectively. He is currently an associate professor with the Faculty of Mechanical Engineering at the University of Tabriz. Dr. Keighobadi's research interests include estimation and control of nonlinear, stochastic and intelligent systems as well as applications in robotic and navigation systems. He has also interests in linear and nonlinear Kalman Filters, MPC, H∞, Fuzyy NNTs, LMI, Machine Learning, Deep learning design and implementation by Linux/Windows based microcontrollers and microprocessor boards.

